Altered axonal architecture by removal of the heavily phosphorylated neurofilament tail domains strongly slows superoxide dismutase 1 mutant-mediated ALS

Christian S. Lobsiger, Michael L. Garcia, Christopher M. Ward*, and Don W. Cleveland†

Ludwig Institute for Cancer Research and Departments of Medicine and Neuroscience, University of California at San Diego, 9500 Gilman Drive, La Jolla, CA 92093

Eliminating assembled neurofilaments (NFs) from axons or misaccumulating NFs in motor neuron cell bodies strongly slows disease in mouse models of mutant superoxide dismutase 1 (SOD1)-induced amyotrophic lateral sclerosis. One proposal for how reducing axonal NFs can increase survival is that the multiphosphorylated tail domains of the two larger NF subunits act in motor neuron cell bodies as phosphorylation sinks where they mitigate cyclin-dependent kinase 5 dysregulation induced by mutant SOD1. Elimination by gene targeting in mice of the NF medium and NF heavy tail domains and their 58 known phosphorylation sites accelerates aberrant phosphorylation of other neuronal substrates while leaving overall NF content unaltered. However, disease onset is significantly delayed and survival is extended, inconsistent with the ameliorative property of altered NF content protecting by serving as substrates for dysregulation of any NF kinase. Moreover, at comparable disease stages significantly more surviving motor neurons and axons were found in SOD1 mutant mice deleted in the NF tails than in similar mice with wild-type NFs. This finding supports noncell autonomous toxicity in SOD1 mutant-mediated amyotrophic lateral sclerosis: removal of the NF tails slows damage developed directly within motor neurons, but SOD1 mutant damage within nonneuronal supporting cells reduces motor neuron functionality.

axonal transport | axonal cytoskeleton | cyclin-dependent kinase 5

Amyotrophic lateral sclerosis (ALS) is an adult-onset neurodegenerative disease that is responsible for ≈1 in 1,000 deaths (1). Dominant missense mutations in the gene for the cytoplasmic Cu/Zn superoxide dismutase 1 (SOD1) are responsible for ≈20% of familial ALS cases (2). Despite the ubiquitous expression of SOD1 (3), mutations in this protein produce a disease that selectively kills upper and lower motor neurons (reviewed in ref. 4). Mice overexpressing mutant SOD1 develop late-onset, ALS-like disease comparable to human ALS (5–7), whereas mice deleted in SOD1 do not (8). This finding has led to the conclusion that mutant SOD1-mediated ALS is caused by an acquired toxicity unrelated to dismutase activity (7, 9). Aberrant oxidative chemistry, mutant aggregation especially onto spinal mitochondria (10), and glutamate excitotoxicity (7, 11) are among the possible hypotheses that have been formulated to explain the toxic property of mutant SOD1 (4). Furthermore, although it is mainly the large motor neurons that die in ALS, mutant SOD1-mediated toxicity is noncell-autonomous, requiring mutant expression within multiple spinal cord cell types (12).

One of the longest-standing hypotheses for a mechanistic contributor to ALS is involvement of abnormal neurofilament (NF) organization. Indeed, aberrant accumulations of NFs are a common pathological hallmark in both sporadic and familial ALS (13–15) as well as in some mutant SOD1 mouse models (5, 16, 17). NFs are obligate heteropolymers of NF light (NF-L), NF medium (NF-M), and NF heavy (NF-H) subunits (18, 19) and are the most abundant structural components of large myelin-

ated axons, the neurons most at risk in human ALS (20) and mutant SOD1 mouse models (7). The large tail domains of NF-M and NF-H are nearly stochiometrically phosphorylated and are responsible for assembly of a 3D, crosslinked axoplasm that supports acquisition of normal axonal caliber (21). Interestingly, accumulation of modest levels of a point mutation in NF-L also produces an ALS-like motor neuron disease in mice (22).

Several prior efforts have altered NF composition in SOD1 mutant mice, including deletion of NF-L in SOD1^{G85R} (23) or SOD1^{G37R} mice (24) and NF-H overexpression in SOD1^{G37R} (25) or SOD1^{G93A} mice (26). Disruption of the NF-L gene removed all axonal NFs, with unassembled NF-M and NF-H subunits accumulated in the neuronal perikaryon. This genetic alteration delayed disease onset and extended survival in SOD1^{G85R} mice by ≈1.5 months, despite the significant disadvantage of loss of ≈15% of motor neurons early in postnatal life in the absence of NFs (23). On the other hand, increased expression of NF-H decreased axonal NF content by trapping most in the motor neuron cell bodies, extending life span in SOD1^{G37R} mice by 3–6.5 months, by far one of the most striking slowings of SOD1-mediated disease to date in mice (24, 25).

Two models have been proposed to explain how altering axonal NFs can alleviate mutant SOD1 toxicity (outlined in Fig. 5, which is published as supporting information on the PNAS web site). In the first, a beneficial effect within the cell bodies has been postulated from the increased perikaryal content of NF-M and NF-H (filamentous or as subunits), whose multiphosphorylation sites in their tail domains could serve as phosphorylation sinks for buffering mutant SOD1-induced hyperactive cyclin-dependent kinase 5 (Cdk5) (24, 25). This first model is based on the finding that slowing of disease after overexpression of NF-H reduced hyperphosphorylation of tau, one of the target proteins of misregulated Cdk5 (24). Although deletion of the neuronal Cdk5 activator p35 does not alter the disease course in mutant SOD1 mice (27), increased phosphorylation of tau (and probably other substrates) during disease progression may arise from sustained action of alternative Cdk5 activators, such as p39 (28), or other mutant SOD1-induced kinases.

An alternative hypothesis (23, 29) has proposed that the protective effect of altering NF content is primarily an axonal one, in which a reduced burden of NFs, especially the interactions mediated by their phosphorylated tail domains, reduces the NF-dependent slowing of slow axonal transport, which has been shown to directly depend on the phosphorylation state of NF-tail

NEUROSCIENCE

domains (30). Because there is a presymptomatic deficit in transit of cargoes of slow axonal transport in mutant SOD1 mice (29), this latter hypothesis predicts that removing NF-M and NF-H tail domains (and all of their known phosphorylation sites) will reduce axonal crosslinking and restore more normal transport.

These two models make very different predictions of what would happen to SOD1-mediated toxicity in mice with normal NF content but missing the NF-M and NF-H tail domains and their phosphorylation sites. If the first hypothesis is correct, disease would be accelerated (or unchanged), whereas the axonal hypothesis predicts slowed mutant SOD1-mediated disease. We have now tested these models by generating and analyzing disease in SOD1^{G37R} mice in which gene replacement was used to remove the tail domains of NF-M, NF-H, or both.

Materials and Methods

Generation of Mutant SOD1 Mice Lacking NF-M/H Tail Domains. Mice overexpressing the mutant human *SOD1* gene (SOD1^{G37R}, line 106) (6) were on a pure C57BL/6 background. Mice lacking both the NF-M and NF-H tail domains [NF-(M/H)$^{tail\Delta}$] were previously generated on a mixed 129SJL/C57BL/6 background (21, 31, 32). The main mating strategy to obtain the NF-(M/H)$^{wild-type}$/SOD1^{G37R} and the NF-(M/H)$^{tail\Delta}$/SOD1^{G37R} mice is shown in Fig. 1A. Additional animals were produced by interbreeding NF-(M/H)$^{tail\Delta}$/SOD1^{G37R}, NF-(M/H)$^{wild-type}$/SOD1^{G37R}, NF-M$^{tail\Delta}$/SOD1^{G37R}, and NF-H$^{tail\Delta}$/SOD1^{G37R} mice to their respective counterparts lacking the mutant SOD1 transgene. Approximately 50% of the animals of each of the six main genotypes (Fig. 1A) were generated by this last method. Average disease onset and end stage were indistinguishable between animals derived from either breeding approach, mitigating concerns regarding possible influences of the mixed genetic backgrounds (data not shown). More than 600 mice were generated, and the number of progeny obtained for each genotype was as expected for Mendelian transmission. Genotyping was performed as described (21, 29). Mice were weighed weekly as an objective measure of disease course. End stage was defined by the inability of an animal to right itself within 20 s when placed on its side.

SDS/PAGE and Immunoblotting. Sciatic nerve and spinal cord protein extracts (both at hind limb weakness) were made and analyzed as described (33). Protein extracts (15 μg) from one to three animals per genotype were separated individually by SDS/PAGE using gels containing 7.5% (NFs and tau) or 12.5% (SOD1) polyacrylamide and transferred to nitrocellulose (34). The NF-L subunit was identified by using an affinity-purified rabbit polyclonal antibody (1/400) (35), whereas human and mouse SOD1 were detected with a rabbit polyclonal antibody (1/1,500) (3). Total tau was detected by a phosphorylation-independent mouse mAb (BioSource International, Camarillo, CA; Tau-5; 1/1,000), whereas phospho-tau was detected by a mouse mAb recognizing an epitope containing the phosphorylated Ser-409 (PG5, a kind gift of Peter Davies, Albert Einstein College of Medicine, Bronx, NY; 1/100). Membranes were incubated with the antibodies as described (21).

Quantitation of Axons, Neurons, and Neuromuscular Junctions. For tissue collection mice were perfused with 4% formaldehyde. Both L5 motor roots from each animal were counted and averaged (21), and axonal caliber distributions were determined as described (21). Spinal cords and gastrocnemius muscles were cryoprotected and snap-frozen in isopropanol in TissueTek (Sakura, Torrance, CA). Thirty-micrometer serial
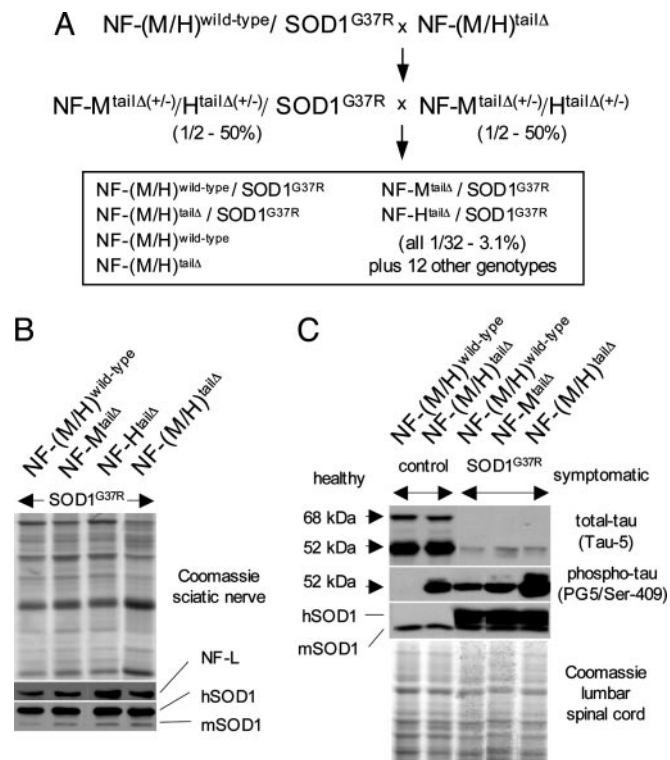

Fig. 1. Generation and immunoblot analysis of mutant SOD1 mice lacking the NF tail domains. (*A*) Mating scheme to obtain the six genotypes followed for this study (boxed) consisting of mutant SOD1 mice (SOD1^{G37R}) with either normal NF content [NF-(M/H)$^{wild-type}$/SOD1^{G37R}] or that are deleted in one or both of the NF tail domains [NF-M$^{tail\Delta}$/SOD1^{G37R}, NF-H$^{tail\Delta}$/SOD1^{G37R}, and NF-(M/H)$^{tail\Delta}$/SOD1^{G37R}], plus the two control genotypes without mutant SOD1 (expected Mendelian frequencies are indicated). (*B*) Parallel immunoblots of sciatic nerve extracts from the four mutant SOD1 mice containing normal or tail domain-deleted NFs, showing unchanged levels of NFs (as determined by NF-L) and of both mouse and mutant human SOD1 proteins (m/hSOD1). (*C*) Parallel immunoblots of spinal cord extracts confirming that the NF-M/H tail domains can act as phosphorylation sinks against Cdk5 targets like tau (see text). Control animals were 6 months old, whereas mutant SOD1 mice were at hind limb weakness. Equal loading is shown by Coomassie and the endogenous mouse SOD1 (mSOD1), whereas total tau was detected with tau-5 and phospho-tau with PG5 antibodies. Note that because overall total tau levels are down-regulated in mutant SOD1 mice (see text) the ratio of phosho/unphospho-tau is actually higher in the NF-(M/H)$^{wild-type}$/SOD1^{G37R} mice than in the control NF-(M/H)$^{tail\Delta}$ mice, although the total phospho-tau level is reduced, consistent with a mutant SOD1-induced deregulation of Cdk5 (24).

spinal cord cryosections were cut between sacral S1 and lumbar L2, and every sixth section was stained with cresyl-violet-acetate (Sigma). A total of 20 lumbar L3–L6 sections per animal were analyzed, and both the total and the large (>25 μm in diameter) ventral horn motor neurons were counted. One gastrocnemius muscle per animal was analyzed, 40-μm serial cryosections were cut, and every 12th section was collected. A total of eight sections per animal were analyzed. Floating sections were blocked with 1.5% bovine albumin in PBS and 0.5% Tween 20 and stained with polyclonal rabbit antibodies against synaptophysin (1/50) (Zymed) and NF-L (1/50) (35) in PBS and 0.3% Triton X-100 for 4 days at 4°C. α-Bungarotoxin coupled to Alexa Fluor 488 (1/250) (Molecular Probes) was added, and antibodies were detected by goat anti-rabbit Cy3-coupled secondary antibodies (1/250) (Jackson ImmunoResearch). End-plate analysis was done on a Olympus confocal microscope using FV1000.

Results

Removal of the NF-M/H Tail Domains Delays Disease Onset and Prolongs the Survival of Mutant SOD1 Mice. NF-(M/H)^{tailΔ} mice have been described in which gene replacement was used to eliminate the tail domains of both NF-M and NF-H (21). These were mated to a mutant SOD1 mouse (SOD1^{G37R}; line 106) that reaches disease end stage by 11.8 months (±0.2 SEM, $n = 12$). Levels of mutant accumulation as well as timing of disease onset and survival were almost identical to the SOD1^{G37R} mouse (line 29), which was used in two prior experiments in which deletion of NF-L (24) or overexpression of NF-H (24, 25) slowed disease. A multistep mating strategy generated mutant SOD1 mice with normal NF content [NF-(M/H)$^{wild-type}$/SOD1^{G37R}] or deleted in the NF-M (NF-M^{tailΔ}/SOD1^{G37R}), NF-H (NF-H^{tailΔ}/SOD1^{G37R}), or both NF tail domains [NF-(M/H)^{tailΔ}/SOD1^{G37R}] with all relevant genotypes in a common set of littermates (Fig. 1A). We have previously shown that deletion of the NF tail domains did not change the levels of the accumulated NF protein subunits (21). Using quantitative immunoblotting for NF-L, the major subunit of assembled NF heteropolymers, we confirmed the unchanged NF levels in sciatic nerve extracts from mutant SOD1 mice with or without the NF-M and/or NF-H tail domains (Fig. 1B). Importantly, removal of the NF tail domains did not affect mutant SOD1 protein levels (Fig. 1B).

Disease onset and progression were documented with multiple measures, including hind limb weakness, leg spread when suspended by the tail, gait abnormalities, and weight loss, the last of which provided a simple, rapid, and objective measure (36, 37). No mice without mutant SOD1 [e.g., NF-(M/H)$^{wild-type}$ or NF-(M/H)^{tailΔ} mice] developed any hind limb symptoms or weight loss by 14 months of age, the oldest age analyzed ($n = 10$ each; data not shown). Four disease stages were defined: presymptomatic (before onset, at 6 months), onset (at the weight peak), hind limb weakness (at 10% weight loss, which was invariably accompanied by alterations in gait, development of tremors, and failure of hind limb splaying when suspended by the tail), and end stage (hind limb paralysis).

In a direct test of the phosphorylation sink hypothesis for NF tail domains in mutant SOD1 mice (24) (Fig. 5), we analyzed the phosphorylation state of tau, a target for Cdk5, in control NF-(M/H)^{tailΔ} and symptomatic NF-(M/H)^{tailΔ}/SOD1^{G37R} mice and compared it with NF-(M/H)$^{wild-type}$ and symptomatic NF-(M/H)$^{wild-type}$/SOD1^{G37R} mice (Fig. 1C). Indeed, phospho-tau (Ser-409) was increased in mice lacking NF tail domains, independent of the presence of mutant SOD1. This effect was true despite an overall down-regulation of total tau in symptomatic SOD1 mutant animals, perhaps reflecting loss of motor neurons. Thus, NF tail domains can and do serve as phosphorylation sinks whose loss is accompanied by increased phosphorylation by NF kinases (including Cdk5) of other neuronal components.

If the increased perikaryal accumulation of NFs (and hence increased buffering for dysregulated kinases) underlies their ability to ameliorate disease, then removing the NF tail domains should increase detrimental hyperphosphorylation of deregulated kinase targets like tau and accelerate mutant SOD1-mediated disease (Fig. 5). Just the opposite was found: NF-(M/H)$^{wild-type}$/SOD1^{G37R} mice reached onset at 7.1 months (±0.2, $n = 17$) before significant loss of motor axons (38) and correlating well with slowing of axonal transport at 6–7 months, the earliest change in these mice that express relatively low levels of SOD1^{G37R} (29). Hind limb weakness was reached at 10.1 months (±0.2, $n = 17$), whereas end stage occurred at 11.8 months (±0.2, $n = 12$).

In contrast, NF-(M/H)^{tailΔ}/SOD1^{G37R} mice did not reach onset until 9.1 months (±0.4, $n = 15$) (Fig. 2A), representing a 2-month delay in disease onset. Likewise, in NF-(M/H)^{tailΔ}/SOD1^{G37R}
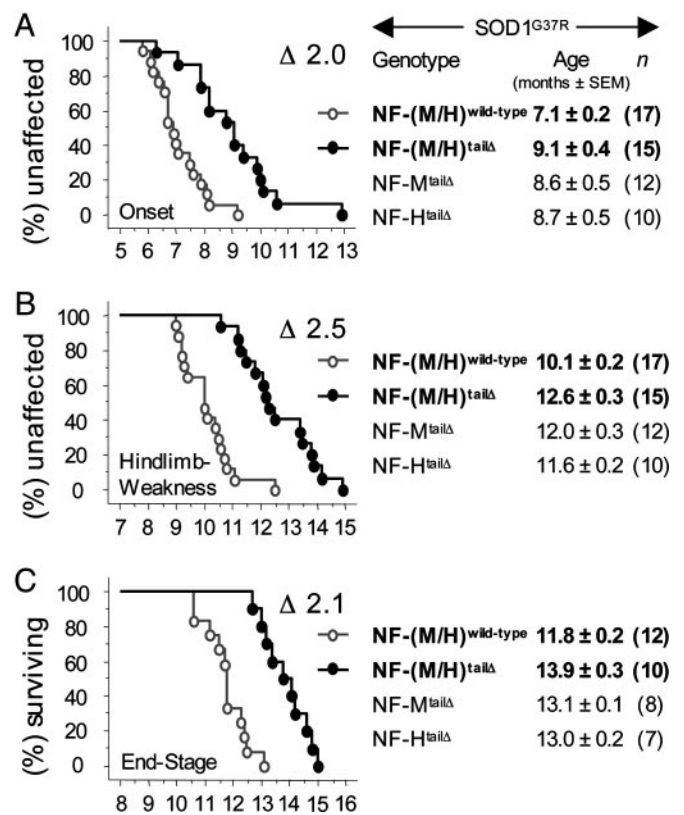
Fig. 2. Removing the NF tail domains delayed disease onset and extended survival in mutant SOD1 mice. Kaplan-Meier curves showing age (and delay Δ in months) of disease onset (weight peak) (A), hind limb weakness (10% weight loss) (B), and end stage (hind limb paralysis) (C) of mutant SOD1 mice with normal or tail domain-deleted NF content. The respective average ages (with SEM and number of animals) are indicated on the right including the mutant SOD1 mice that had only one NF tail domain deleted.

mice hind limb weakness was delayed 2.5 months, occurring at 12.6 months (±0.3, $n = 15$), a time when most of the NF-(M/H)$^{wild-type}$/SOD1^{G37R} mice had already died (Fig. 2B). NF-(M/H)^{tailΔ}/SOD1^{G37R} mice reached end stage at 13.9 months (±0.3, $n = 10$), 2.1 months later than NF-(M/H)$^{wild-type}$/SOD1^{G37R} mice (Fig. 2C). All three delays reached high statistical significance (using ANOVA and Bonferroni/Dunn post hoc test: $P < 0.0002$). Delay from loss of the tail domains was additive: mice deleted in only one of the two NF tail domains showed smaller, but still significant, delays in all three measured disease stages (Fig. 2).

Motor Neurons Lacking the NF-M/H Tail Domains Are Protected Against Mutant SOD1 Toxicity. To determine whether at similar disease stages the extent of neurodegeneration was the same in animals with or without NF tail domains, lumbar (L5) motor (ventral) roots were examined and all axons within them were counted. Despite decreased axonal calibers in NF-(M/H)^{tailΔ} mice relative to mice with wild-type NFs (as reported earlier) (21), both at hind limb weakness and end stage, there were significantly more surviving axons in the NF-(M/H)^{tailΔ}/SOD1^{G37R} mice relative to those in the NF-(M/H)$^{wild-type}$/SOD1^{G37R} animals (Fig. 3 A–F). This difference was statistically significant (using ANOVA and Fisher's probable least-squares difference post hoc test: $P < 0.0065$) and resulted at hind limb weakness in 40% and at end stage in 64% more surviving axons for NF-(M/H)^{tailΔ}/SOD1^{G37R} mice than for NF-(M/H)$^{wild-type}$/SOD1^{G37R} animals (Fig. 3G). The absolute number of remaining L5 motor axons found in NF-(M/H)^{tailΔ}/SOD1^{G37R} mice at hind

NEUROSCIENCE
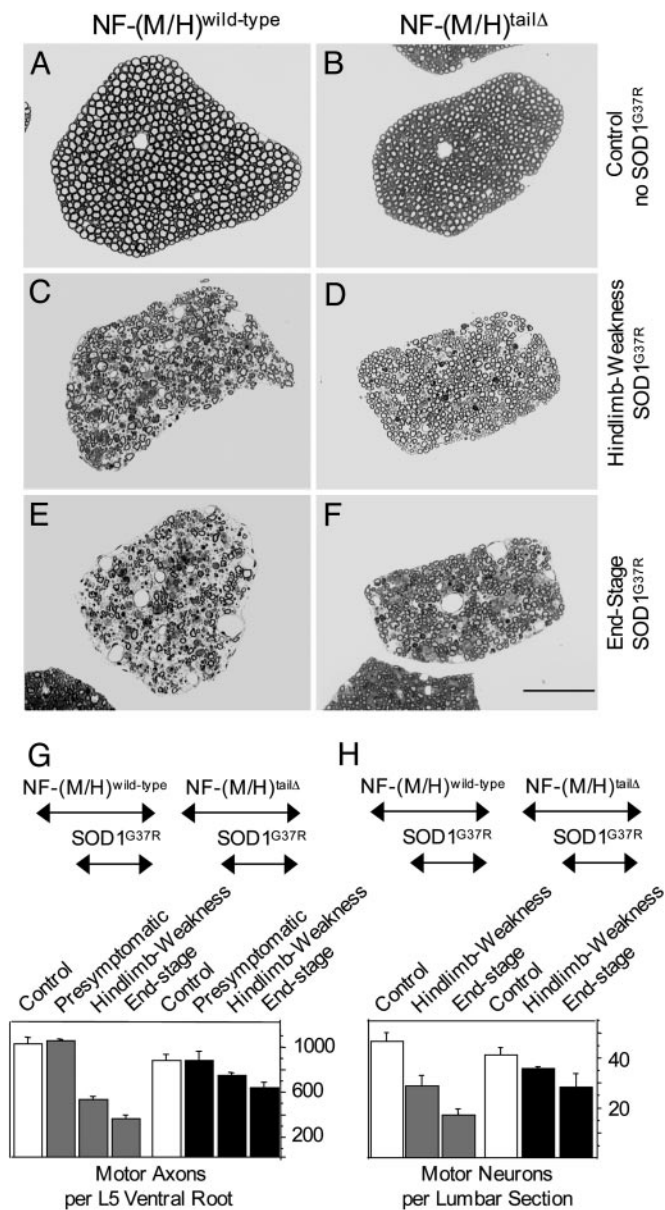
Fig. 3. Mutant SOD1-induced loss of motor neurons is reduced in mice lacking both NF tail domains despite similar disease stages. (*A–F*) L5 ventral root axons of control mice without mutant SOD1 with no obvious axonal degeneration at 14 months of age (*A* and *B*) and mutant SOD1 mice with normal (*C* and *E*) or tail domain-deleted (*D* and *F*) NF content both at hind limb weakness (*C* and *D*) and end stage (*E* and *F*). (Scale bar: 200 μm, *F*.) (*G* and *H*) Quantitative analysis of the loss of L5 ventral root axons (*G*) and total L3-L6 lumbar ventral horn motor neuron cell bodies (*H*) [error bars are SEM; $n = 3–4$ animals for axon and neuron counts, except for neurons in end stage NF-(M/H)$^{tail\Delta}$/SOD1^{G37R} mice where $n = 2$]. Mice were analyzed before onset (presymptomatic, at 6 months), at hind limb weakness, and at end stage. Control mice without mutant SOD1 were analyzed at 14 months.

limb weakness was 72% (724 ± 26 axons; $n = 3$) of 14-month-old control NF-(M/H)$^{wild-type}$ animals (1,008 ± 61 axons; $n = 3$). In contrast, at the same disease stage, NF-(M/H)$^{wild-type}$/ SOD1^{G37R} mice had only 51% (517 ± 29 axons; $n = 4$) surviving axons. Similarly, by end stage NF-(M/H)$^{tail\Delta}$/SOD1^{G37R} mice had 61% (613 ± 51 axons; $n = 3$) of the normal number of axons, whereas NF-(M/H)$^{wild-type}$/SOD1^{G37R} mice had many fewer, only 37% (374 ± 29 axons; $n = 4$) (Fig. 3*G* and Table 1, which is published as supporting information on the PNAS web site).

Even more surprisingly, end-stage NF-(M/H)$^{tail\Delta}$/SOD1^{G37R} mice not only showed more surviving axons than did end-stage NF-(M/H)$^{wild-type}$/SOD1^{G37R} mice, they retained more than NF-(M/H)$^{wild-type}$/SOD1^{G37R} mice at the earlier hind limb weakness stage (Fig. 3*G*). This outcome was true despite a slight reduction in axonal numbers (15% less; $P = 0.0457$) in NF-(M/H)$^{tail\Delta}$ mice and presymptomatic NF-(M/H)$^{tail\Delta}$/SOD1^{G37R} mice relative to the NF wild-type animals both in the presence (presymptomatic) and absence of SOD1^{G37R} (Fig. 3*G* and Table 1).

Because interpretation of axonal numbers in motor roots could be confounded by potential proximal sprouting, L3–L6 ventral horn motor neurons were also counted. Consistent with the axon numbers, there were more surviving motor neurons at similar disease stages in the NF-(M/H)$^{tail\Delta}$/SOD1^{G37R} mice as compared with the NF-(M/H)$^{wild-type}$/SOD1^{G37R} mice [77% and 61% at hind limb weakness and end stage, respectively, whereas only 62% and 37% remained in NF-(M/H)$^{wild-type}$/SOD1^{G37R} mice; Fig. 3*H* and Table 1; all compared with control NF-(M/H)$^{wild-type}$ mice]. This finding was even more pronounced for the larger ventral horn motor neurons with perikaryal diameters >25 μm [at hind limb weakness, 69% of those in wild-type mice remained in NF-(M/H)$^{tail\Delta}$/SOD1^{G37R} spinal cords versus 45% in NF-(M/H)$^{wild-type}$/SOD1^{G37R}; Table 1]. Comparable to the slight reduction of the number of L5 ventral root axons in control NF-(M/H)$^{tail\Delta}$ mice as compared with NF-(M/H)$^{wild-type}$ mice, there were also slighter fewer ventral horn motor neurons in control NF-(M/H)$^{tail\Delta}$ mice, although the difference did not reach statistical significance (ANOVA and Fisher's probable least-squares difference post hoc test; 11% less; $P = 0.255$) (Fig. 3 *G* and *H* and Table 1). Nevertheless, the robust extension in lifespan in NF-(M/H)$^{tail\Delta}$/SOD1^{G37R} mice compared with NF-(M/H)$^{wild-type}$/SOD1^{G37R} mice came despite fewer initial axons and neurons in control NF-(M/H)$^{tail\Delta}$ mice as compared with control NF-(M/H)$^{wild-type}$ mice.

At Similar Disease Stages Mutant SOD1-Mediated Axonal Degeneration Is Slowed in Mice Lacking the NF Tail Domains. Because at similar disease stages the NF-(M/H)$^{tail\Delta}$/SOD1^{G37R} mice had more axons and surviving motor neurons than NF-(M/H)$^{wild-type}$/SOD1^{G37R} mice, we assessed two additional parameters to more directly test the functionality of these remaining motor neurons: retention of axonal caliber and the integrity of surviving neuromuscular junctions. In presymptomatic mice before onset, the axon caliber distribution in both the NF-(M/H)$^{wild-type}$/SOD1^{G37R} and the NF-(M/H)$^{tail\Delta}$/SOD1^{G37R} mice were as in their respective control animals without mutant SOD1 (Fig. 4*A*). At hind limb weakness NF-(M/H)$^{wild-type}$/SOD1^{G37R} mice retained 51% of their L5 ventral root axons (Fig. 3*G*), with essentially all of the loss arising from the pool of larger caliber axons (Fig. 4*A*). In contrast, at the same disease stage, NF-(M/H)$^{tail\Delta}$/SOD1^{G37R} mice still had 72% of their axons remaining (Fig. 3*G*) and a bimodal caliber distribution essentially the same as in the control NF-(M/H)$^{tail\Delta}$ animals (Fig. 4*A*). Finally, at end stage with still 61% remaining axons in the NF-(M/H)$^{tail\Delta}$/SOD1^{G37R} mice this bimodal distribution was reduced but still partly present, with the main loss in the large-caliber axons (Fig. 4*A*). Thus, although the axonal degeneration is slowed in NF-(M/H)$^{tail\Delta}$/SOD1^{G37R} mice, in both NF-(M/H)$^{wild-type}$ and NF-(M/H)$^{tail\Delta}$ mice SOD1 mutant toxicity produced losses only of the larger-caliber axons even at end stage.

The percentage of innervation remaining was determined at the end plates of neuromuscular junctions of the gastrocnemius, one of the affected hind limb muscles and innervated by L3–L5 spinal nerves. This process revealed robust denervation at the hind limb weakness stage in the NF-(M/H)$^{wild-type}$/SOD1^{G37R} mice, with only 25% remaining innervated end plates (Fig. 4*B*). However, at the same disease stage, more than twice as many (60%) of all analyzed end plates were still innervated in the

A

NF-(M/H)$^{\text{wild-type}}$/SOD1^{G37R} ●   NF-(M/H)$^{\text{wild-type}}$ ○
NF-(M/H)$^{\text{tail}\Delta}$/SOD1^{G37R} ■   NF-(M/H)$^{\text{tail}\Delta}$ □

B

NF-(M/H)$^{\text{wild-type}}$ NF-(M/H)$^{\text{tail}\Delta}$

SOD1^{G37R}

Syn/NF/BTX

Fig. 4. Mutant SOD1 mice lacking both NF tail domains showed a slowing of axonal degeneration and reduced muscle denervation. (*A*) L5 ventral root axon caliber distributions before onset (presymptomatic, at 6 months), at hind limb weakness, and at end stage with normal or tail domain-deleted NF content and with or without mutant SOD1. Points represent the averaged distributions of diameters from three to four animals. Control mice without mutant SOD1 were analyzed at 14 months of age. (*B*) Determination of the percentage of innervated endplates in the gastrocnemius hind limb muscle. (*Left*) Quantitative analysis of denervation in mutant SOD1 mice with or without NF tail domains and in 14-month-old control animals without mutant SOD1. Shown are averages with SEM ($n = 3$ animals; ≈150 bungarotoxin-positive end plates per animal were randomly chosen and analyzed). (*Right*) α-Bungarotoxin (BTX, green) was used to identify the postsynaptic domain, whereas NF (red) and synaptophysin (Syn, red) were used to identify axons and presynaptic terminals. (*Upper*) Yellow area of overlap identifies innervated end plates, while (*Lower*) partly innervated or completely denervated end plates show only green α-bungarotoxin staining. (Scale bar: 50 μm.)

NF-(M/H)$^{\text{tail}\Delta}$/SOD1^{G37R} mice, a difference that was highly significant (using ANOVA and Fisher's probable least-squares difference post hoc test: $P = 0.0082$) (Fig. 4*B* and Table 1). Even more surprisingly, this trend was preserved even at end stage,

with still two times more innervated neuromuscular junctions in the NF-(M/H)$^{\text{tail}\Delta}$/SOD1^{G37R} mice as compared with the NF-(M/H)$^{\text{wild-type}}$/SOD1^{G37R} mice (25 vs. 13%, respectively; Fig. 4*B* and Table 1).

Discussion

We have shown that the removal of the large phosphorylated tail domains of NF-M and NF-H delays disease onset and extends survival of mutant SOD1 mice by 2 months, coupled to a partial protection of the entire motor neuron unit (cell body, axon, and end plate). The ameliorative effects on onset and survival are similar in magnitude to those produced by eliminating axonal NF assembly altogether (by deletion of the NF-L gene) (23). Further, we showed that NF tail domains can act as phosphorylation sinks that minimize phosphorylation by Cdk5 or other NF kinases. Nevertheless, removal of these phosphorylation sites led to a delay of disease rather than the acceleration predicted by a kinase dysregulation model. Clearly, the multiphosphorylation sites on both NF-M and NF-H, and hence the possibility that they could act as phosphorylation sinks to mitigate dysregulated Cdk5 (or any other NF kinase), are not an essential mechanistic contributor to diminished toxicity of ALS-causing SOD1 mutants in mice of altered NF subunit composition.

What then can explain the beneficial effect of removing NFs from the axons? Removal of the large, multiply phosphorylated NF tail domains produces smooth, wavy NFs lacking most of the numerous cross bridges between adjacent NFs and microtubules (21). Furthermore, the reduction of axonal NF content and the removal of the NF-H tail domain has been shown to accelerate the net rate of movement of cargoes in slow axonal transport (31, 39–41). Site-directed mutation to produce nonphosphorylatable NFs or mimic constitutive phosphorylation in primary neurons has been shown to accelerate or retard transport, respectively (30). On the other hand, SOD1 mutants have been shown to inhibit movement of slow axonal transport cargoes beginning at presymptomatic disease stages (29). Mutant SOD1 action may also inhibit retrograde transport, as indicated by a striking distal accumulation of mitochondria and synaptic vesicles at the pre-synaptic terminals of motor neurons (42). Collectively, these data identify establishment of a more flexible axoplasm that can enhance anterograde transport as one mechanism underlying the benefit of removing the NF-M and NF-H tail domains in SOD1 mutant-mediated motor neuron disease.

The robust benefit in slowing SOD1 mutant-mediated disease in NF-(M/H)$^{\text{tail}\Delta}$/SOD1^{G37R} mice was found to a lesser degree in mice lacking either one of the NF tail domains (NF-M$^{\text{tail}\Delta}$/SOD1^{G37R} and NF-H$^{\text{tail}\Delta}$/SOD1^{G37R} mice), indicating an additive effect of deleting both NF tail domains. However, and quite surprisingly, there was an additional neuroprotection resulting in many more surviving motor neuron units at a similar disease stage as compared with the initial mutant SOD1 mice with normal NF content. This motor neuron sparing, both in axon number and caliber distribution, required deletion of both NF-M and NF-H tail domains (Table 1 and data not shown).

These findings raise a perplexing question in the mechanism of SOD1 mutant-mediated disease: how can a similar clinical deficit, such as hind limb weakness or hind limb paralysis be generated despite different numbers of surviving motor neuron units? Removal of the NF tail domains protects motor neurons against mutant SOD1 toxicity, slows disease, and preserves more neurons even as paralysis ensues. It also slows axonal degeneration, including synaptic retraction, an event proposed to be one of the earliest in mutant SOD1-mediated ALS in mice (43), even though function is not preserved. Thus, removal of the NF tail domains reveals that mutant SOD1 motor neurons lose functionality before obvious signs of denervation and axonal degeneration. Interestingly, a similar phenomenon was recently reported in mutant SOD1 mice that were treated with a virus to

produce RNA interference to lower synthesis and accumulation of mutant SOD1. Viral injection into muscles and subsequent retrograde transport to the motor neuron cell bodies yielded mice that survived much longer than untreated controls, but just as we have found here, when these animals ultimately reach end stage they retained an increased number of surviving motor neurons when compared with control animals (44).

In this respect it is of interest that analysis of chimeric mice that are a mixture of wild-type and SOD1 mutant-expressing cells have been used to demonstrate that toxicity is noncell autonomous (12), with mutant action within nonneuronal cells required for neuronal loss. Disease stage may thus be determined by the collective damage from mutant SOD1 action within multiple cell types, especially those neighboring the motor neurons, including astrocytes, microglia, Schwann cells, and the muscle cells to which they attach. For NFs, the simplest view is

that because NF-M and NF-H are preferentially expressed in large, myelinated motor neurons, removal of the NF tail domains has a direct influence only on those neurons, whereas damage in the nonneuronal cells progresses unabated. Thus, a local protective effect from removing the NF tail domains slows pathology within the motor neuron, whereas a strong toxic environment reduces its functionality.

1. Mulder, D. W., Kurland, L. T., Offord, K. P. & Beard, C. M. (1986) *Neurology* **36,** 511–517.
2. Rosen, D. R., Siddique, T., Patterson, D., Figlewicz, D. A., Sapp, P., Hentati, A., Donaldson, D., Goto, J., O'Regan, J. P., Deng, H. X., *et al*. (1993) *Nature* **362,** 59–62.
3. Pardo, C. A., Xu, Z., Borchelt, D. R., Price, D. L., Sisodia, S. S. & Cleveland, D. W. (1995) *Proc. Natl. Acad. Sci. USA* **92,** 954–958.
4. Bruijn, L. I., Miller, T. M. & Cleveland, D. W. (2004) *Annu. Rev. Neurosci.* **27,** 723–749.
5. Gurney, M. E., Pu, H., Chiu, A. Y., Dal Canto, M. C., Polchow, C. Y., Alexander, D. D., Caliendo, J., Hentati, A., Kwon, Y. W., Deng, H. X., *et al*. (1994) *Science* **264,** 1772–1775.
6. Wong, P. C., Pardo, C. A., Borchelt, D. R., Lee, M. K., Copeland, N. G., Jenkins, N. A., Sisodia, S. S., Cleveland, D. W. & Price, D. L. (1995) *Neuron* **14,** 1105–1116.
7. Bruijn, L. I., Becher, M. W., Lee, M. K., Anderson, K. L., Jenkins, N. A., Copeland, N. G., Sisodia, S. S., Rothstein, J. D., Borchelt, D. R., Price, D. L., *et al*. (1997) *Neuron* **18,** 327–338.
8. Reaume, A. G., Elliott, J. L., Hoffman, E. K., Kowall, N. W., Ferrante, R. J., Siwek, D. F., Wilcox, H. M., Flood, D. G., Beal, M. F., Brown, R. H., Jr., *et al*. (1996) *Nat. Genet.* **13,** 43–47.
9. Bruijn, L. I., Houseweart, M. K., Kato, S., Anderson, K. L., Anderson, S. D., Ohama, E., Reaume, A. G., Scott, R. W. & Cleveland, D. W. (1998) *Science* **281,** 1851–1854.
10. Liu, J., Lillo, C., Jonsson, P. A., Vande Velde, C., Ward, C. M., Miller, T. M., Subramaniam, J. R., Rothstein, J. D., Marklund, S., Andersen, P. M., *et al*. (2004) *Neuron* **43,** 5–17.
11. Howland, D. S., Liu, J., She, Y., Goad, B., Maragakis, N. J., Kim, B., Erickson, J., Kulik, J., DeVito, L., Psaltis, G., *et al*. (2002) *Proc. Natl. Acad. Sci. USA* **99,** 1604–1609.
12. Clement, A. M., Nguyen, M. D., Roberts, E. A., Garcia, M. L., Boillee, S., Rule, M., McMahon, A. P., Doucette, W., Siwek, D., Ferrante, R. J., *et al*. (2003) *Science* **302,** 113–117.
13. Hirano, A., Nakano, I., Kurland, L. T., Mulder, D. W., Holley, P. W. & Saccomanno, G. (1984) *J. Neuropathol. Exp. Neurol.* **43,** 471–480.
14. Hirano, A., Donnenfeld, H., Sasaki, S. & Nakano, I. (1984) *J. Neuropathol. Exp. Neurol.* **43,** 461–470.
15. Hirano, A. (1991) *Adv. Neurol.* **56,** 91–101.
16. Tu, P. H., Raju, P., Robinson, K. A., Gurney, M. E., Trojanowski, J. Q. & Lee, V. M. (1996) *Proc. Natl. Acad. Sci. USA* **93,** 3155–3160.
17. Morrison, B. M., Gordon, J. W., Ripps, M. E. & Morrison, J. H. (1996) *J. Comp. Neurol.* **373,** 619–631.
18. Ching, G. Y. & Liem, R. K. (1993) *J. Cell. Biol.* **122,** 1323–1335.
19. Lee, M. K. & Cleveland, D. W. (1996) *Annu. Rev. Neurosci.* **19,** 187–217.
20. Kawamura, Y., Dyck, P. J., Shimono, M., Okazaki, H., Tateishi, J. & Doi, H. (1981) *J. Neuropathol. Exp. Neurol.* **40,** 667–675.
21. Garcia, M. L., Lobsiger, C. S., Shah, S. B., Deerinck, T. J., Crum, J., Young, D., Ward, C. M., Crawford, T. O., Gotow, T., Uchiyama, Y., *et al*. (2003) *J. Cell. Biol.* **163,** 1011–1020.
22. Lee, M. K., Marszalek, J. R. & Cleveland, D. W. (1994) *Neuron* **13,** 975–988.
23. Williamson, T. L., Bruijn, L. I., Zhu, Q., Anderson, K. L., Anderson, S. D., Julien, J. P. & Cleveland, D. W. (1998) *Proc. Natl. Acad. Sci. USA* **95,** 9631–9636.
24. Nguyen, M. D., Lariviere, R. C. & Julien, J. P. (2001) *Neuron* **30,** 135–147.
25. Couillard-Despres, S., Zhu, Q., Wong, P. C., Price, D. L., Cleveland, D. W. & Julien, J. P. (1998) *Proc. Natl. Acad. Sci. USA* **95,** 9626–9630.
26. Kong, J. & Xu, Z. (2000) *Neurosci. Lett.* **281,** 72–74.
27. Takahashi, S. & Kulkarni, A. B. (2004) *J. Neurochem.* **88,** 1295–1304.
28. Tang, D., Yeung, J., Lee, K. Y., Matsushita, M., Matsui, H., Tomizawa, K., Hatase, O. & Wang, J. H. (1995) *J. Biol. Chem.* **270,** 26897–26903.
29. Williamson, T. L. & Cleveland, D. W. (1999) *Nat. Neurosci.* **2,** 50–56.
30. Ackerley, S., Thornhill, P., Grierson, A. J., Brownlees, J., Anderton, B. H., Leigh, P. N., Shaw, C. E. & Miller, C. C. (2003) *J. Cell. Biol.* **161,** 489–495.
31. Rao, M. V., Garcia, M. L., Miyazaki, Y., Gotow, T., Yuan, A., Mattina, S., Ward, C. M., Calcutt, N. A., Uchiyama, Y., Nixon, R. A. & Cleveland, D. W. (2002) *J. Cell. Biol.* **158,** 681–693.
32. Rao, M. V., Campbell, J., Yuan, A., Kumar, A., Gotow, T., Uchiyama, Y. & Nixon, R. A. (2003) *J. Cell. Biol.* **163,** 1021–1031.
33. Rao, M. V., Houseweart, M. K., Williamson, T. L., Crawford, T. O., Folmer, J. & Cleveland, D. W. (1998) *J. Cell. Biol.* **143,** 171–181.
34. Lopata, M. A. & Cleveland, D. W. (1987) *J. Cell. Biol.* **105,** 1707–1720.
35. Xu, Z., Cork, L. C., Griffin, J. W. & Cleveland, D. W. (1993) *Cell* **73,** 23–33.
36. Kieran, D., Kalmar, B., Dick, J. R., Riddoch-Contreras, J., Burnstock, G. & Greensmith, L. (2004) *Nat. Med.* **10,** 402–405.
37. Liu, J., Shinobu, L. A., Ward, C. M., Young, D. & Cleveland, D. W. (2005) *J. Neurochem.* **93,** 875–882.
38. Lariviere, R. C., Beaulieu, J. M., Nguyen, M. D. & Julien, J. P. (2003) *Neurobiol. Dis.* **13,** 158–166.
39. Marszalek, J. R., Williamson, T. L., Lee, M. K., Xu, Z., Hoffman, P. N., Becher, M. W., Crawford, T. O. & Cleveland, D. W. (1996) *J. Cell. Biol.* **135,** 711–724.
40. Zhu, Q., Lindenbaum, M., Levavasseur, F., Jacomy, H. & Julien, J. P. (1998) *J. Cell. Biol.* **143,** 183–193.
41. Shea, T. B., Jung, C. & Pant, H. C. (2003) *Trends Neurosci.* **26,** 397–400.
42. Vande Velde, C., Garcia, M. G., Yin, X., Trapp, B. D. & Cleveland, D. W. (2004) *NeuroMol. Med.* **5,** 193–203.
43. Fischer, L. R., Culver, D. G., Tennant, P., Davis, A. A., Wang, M., Castellano-Sanchez, A., Khan, J., Polak, M. A. & Glass, J. D. (2004) *Exp. Neurol.* **185,** 232–240.
44. Ralph, G. S., Radcliffe, P. A., Day, D. M., Carthy, J. M., Leroux, M. A., Lee, D. C., Wong, L. F., Bilsland, L. G., Greensmith, L., Kingsman, S. M., *et al*. (2005) *Nat. Med.* **11,** 429–433.